Proc. Natl. Acad. Sci. USA
Vol. 87, pp. 7145–7149, September 1990
Medical Sciences

Transgenic mouse model of the mild dominant form of osteogenesis imperfecta

(*Mov-13* mice/osteogenesis imperfecta type I/regulatory collagen mutation)

JEFFREY BONADIO*†‡, THOMAS L. SAUNDERS*, EUGENE TSAI§, STEVEN A. GOLDSTEIN§, JOYCE MORRIS-WIMAN¶, LINDA BRINKLEY¶, DAVID F. DOLAN‖, RICHARD A. ALTSCHULER‖, JOSEPH E. HAWKINS, JR.‖, JOHN F. BATEMAN**, THOMAS MASCARA**, AND RUDOLF JAENISCH††

*Howard Hughes Medical Institute, Departments of †Pathology, §Surgery, and ¶Anatomy and Cell Biology, and ‖Kresge Hearing Research Institute, The University of Michigan, Ann Arbor, MI 48109-0650; **Department of Pediatrics, University of Melbourne, Parkville, Victoria, 3052, Australia; and ††Department of Biology, Whitehead Institute for Biomedical Research, Massachusetts Institute of Technology, Nine Cambridge Center, Cambridge, MA 02142

Communicated by Salome G. Waelsch, June 8, 1990

ABSTRACT **Osteogenesis imperfecta type I is a mild, dominantly inherited, connective tissue disorder characterized by bone fragility. Mutations in type I collagen account for all known cases. In *Mov-13* mice, integration of a murine retrovirus within the first intron of the α1(I) collagen gene results in a null allele blocked at the level of transcription. This study demonstrates that mutant mice heterozygous for the null allele are a model of osteogenesis imperfecta type I. A defect in type I collagen production is associated with dominant-acting morphological and functional defects in mineralized and nonmineralized connective tissue and with progressive hearing loss. The model provides an opportunity to investigate the effect of a reduced amount of type I collagen on the structure and integrity of extracellular matrix. It also may represent a system in which therapeutic strategies to strengthen connective tissue can be developed.**

Osteogenesis imperfecta type I (OI-I) is a mild disorder characterized by bone fracture without deformity, blue sclerae, normal or near normal stature, and autosomal dominant inheritance (1, 2). The incidence is estimated to be 1 of 20,000 live births, and males and females are affected equally. Osteopenia is associated with an increased rate of long-bone fracture upon ambulation. For reasons not well understood, fracture frequency decreases dramatically at puberty and during young adult life but increases once again in late middle age (3). Progressive hearing loss, often beginning in the second or third decade, is a feature of this disease in about half of the families (4). The proportion of OI-I patients with significant hearing loss rises steadily into middle age despite the general decline in fracture frequency. Conductive or mixed (conductive and sensorineural) hearing loss is more common in dominant OI than sensorineural hearing loss alone. Dentinogenesis imperfecta is observed in a small subset of the patient population (5).

All OI-I cases to date have been associated with mutations in the extracellular matrix molecule type I collagen (6). There is evidence that both null alleles and structural mutations can produce this phenotype. Structural alterations within or near the triple-helical domain of collagen chains have been reported (7–11) but appear to represent the minority of cases. Although null OI-I alleles are thought to be common, only one has been characterized at the molecular level (12). As a result, the nature of mutations responsible for the OI-I phenotype is largely unknown, and the pathogenesis of this disease remains poorly understood.

The publication costs of this article were defrayed in part by page charge payment. This article must therefore be hereby marked "*advertisement*" in accordance with 18 U.S.C. §1734 solely to indicate this fact.

The *Mov-13* strain was generated by exposing mouse embryos to Moloney murine leukemia virus. Genetic and molecular evidence indicated that a single copy of the provirus integrated into the first intron of the α1(I) collagen gene (13, 14). The proviral insert is associated with a change in chromatin conformation and *de novo* methylation of the gene, and it prevents initiation of transcription (15–17). Mice homozygous for the null mutation die *in utero* because of failure of the vascular system (18). However, heterozygous *Mov-13* mice (referred to in this paper simply as *Mov-13* mice) do not display an obvious mutant phenotype. Given the nature of the mutation harbored by *Mov-13* mice, it was hypothesized that they would serve as a model of OI-I. In the present report we have undertaken a detailed biochemical and functional analysis of *Mov-13* mice to determine if this were the case.

MATERIALS AND METHODS

Determination of Collagen Content in Skin. Abdominal skin samples taken from littermate wild-type and *Mov-13* female mice (15 weeks) were minced, and skin proteins were extracted sequentially at 4°C into a neutral pH salt buffer and then 0.5 M acetic acid as described (19). Supernatants were dialyzed against 0.5 M acetic acid and quantitated by UV absorbance (215 nm) and also by the Bradford assay (Bio-Rad). Equal aliquots of total protein were treated with pepsin and lyophilized. Serial 1:1 dilutions (12.0–3.0 μg) of wild-type and *Mov-13* samples were resuspended in electrophoresis buffer and separated on SDS/5% PAGE. Gels were fixed in methanol/acetic acid as described (20) and stained with silver according to the manufacturer's recommendations (Bio-Rad). Band identification was by cyanogen bromide peptide mapping (20).

The hydroxyproline content of skin from wild-type and *Mov-13* mice (males and females at 8 weeks) was determined from site-matched, 4-mm circular biopsies of frozen skin. The samples were defatted in chloroform/methanol (2:1, vol/vol) and then hydrolyzed in 6 M HCl under N_2 at 110°C for 20 hr. The dried hydrolysates were analyzed for hydroxyproline content as described (21). Collagen content was calculated by taking into account the normal hydroxyproline content of collagen, based on amino acid analysis, and was expressed as μg of collagen per mm^2 of the original biopsy. All measurements were carried out in duplicate.

Fibroblast Cell Lines and Radiolabeling of Cellular Proteins. Explants of littermate wild-type and *Mov-13* dermal fibroblasts (15-week mice) were prepared and propagated (20).

Abbreviations: OI-I, osteogenesis imperfecta type I; dB, decibels.

‡To whom reprint requests should be addressed.

Radiolabeling of cellular proteins, preparation of pepsin-treated samples, and electrophoresis were performed as described (20).

Bright-Field Microscopy. Littermate wild-type and *Mov-13* abdominal skin specimens were fixed in 2.5% glutaraldehyde in phosphate buffer containing 2% (wt/vol) tannic acid for 6 hr at room temperature. The tissues then were rinsed in buffer, treated with osmium tetroxide, dehydrated by a graded ethanol series, and embedded in Spurr resin (Ted Pella, Tustin, CA). Sections (5 μm) were stained with toluidine blue and photographed with a Leitz Orthoplan microscope (×25 objective).

Biomechanical Studies. After sacrifice, long bones were disarticulated and cleaned of soft tissue. Samples were stored at −30°C prior to analysis. Right whole-bone specimens (humeri and femurs) were obtained from seven wild-type and five *Mov-13* females. Specimens were potted in methyl methacrylate and then stressed to failure in bending on a servohydraulic testing system (model 1000, Instron). The bones were loaded at a constant rate of 0.5 mm/sec until failure occurred, and the ultimate failure load [Newtons (N)], energy to failure (N × mm), and stiffness (N/mm) were determined. Thin sections from cortical bone specimens described above were prepared under constant irrigation by using an Isomet low-speed diamond saw (22). Each section was then milled to a rectangular, parallelepiped beam of tissue that maintained normal osteonal orientation. Specimen geometry was determined from direct video digitization under microscopic examination, and the final dimensions of the rectangular beam specimens typically were 120 × 120 × 1200 μm. A three-point bending stress test was chosen because of specimen size. The beam specimens were loaded at a constant displacement rate of 0.081 mm/sec until failure occurred. Cortical beam displacement was measured by a linear variable differential transformer, and force and deflection data were acquired directly by using an analog to digital converter and a Zenith 286 microcomputer. An effective modulus (gigapascals) was calculated as described (22).

Polarized Light Microscopy. Littermate wild-type and *Mov-13* long bones (humerus and femur) were decalcified and embedded in paraffin. Sections were stained with hematoxylin and eosin. Polarized light microscopy was performed with a Leitz Laborlux 12 Pol microscope (×25 objective).

Hearing. Tone bursts (1.0-ms rise–fall time, 15-ms duration) were presented via a 1.27 cm condenser microphone placed in the external auditory canal within 3–4 mm of the tympanic membrane of the anesthetized mouse (23). The evoked auditory brainstem response (ABR) was differentially recorded from three subcutaneous electrodes placed below each pinna and at the vertex. The amplified (×1000) output from the electrode array was sent to a PC-AT-type computer for averaging (512 samples, 25-msec bin width, 256 responses).

RESULTS

To estimate the amount of collagen in a nonmineralized connective tissue, protein extracts from skin were prepared and equal aliquots were analyzed by gel electrophoresis after treating the samples with pepsin. Pepsin treatment of samples was used prior to electrophoresis to reduce the background of noncollagenous matrix proteins in the extracts. As expected, type I collagen from skin migrated as monomeric (α), dimeric (β), and trimeric (γ) forms because of the presence of crosslinks that persist despite sample preparation and electrophoresis. The amount of type I collagen extracted from *Mov-13* skin was obviously decreased (Fig. 1*A*). This observation was supported by three independent lines of evidence. First, and as anticipated (26, 27), *Mov-13* skin fibroblasts produced half the normal amount of radiolabeled type I collagen in cell culture (Fig. 1*B*). Second, the dermis of *Mov-13* mice contained unusually thin collagen fibers (Fig. 1*C*). The presence of type I collagen in the abnormal fibers was confirmed by an indirect immunofluorescence study that utilized a polyclonal antibody against mouse type I collagen (L.B., unpublished observations). Third, the collagen content of *Mov-13* dermis (as calculated from assays of total

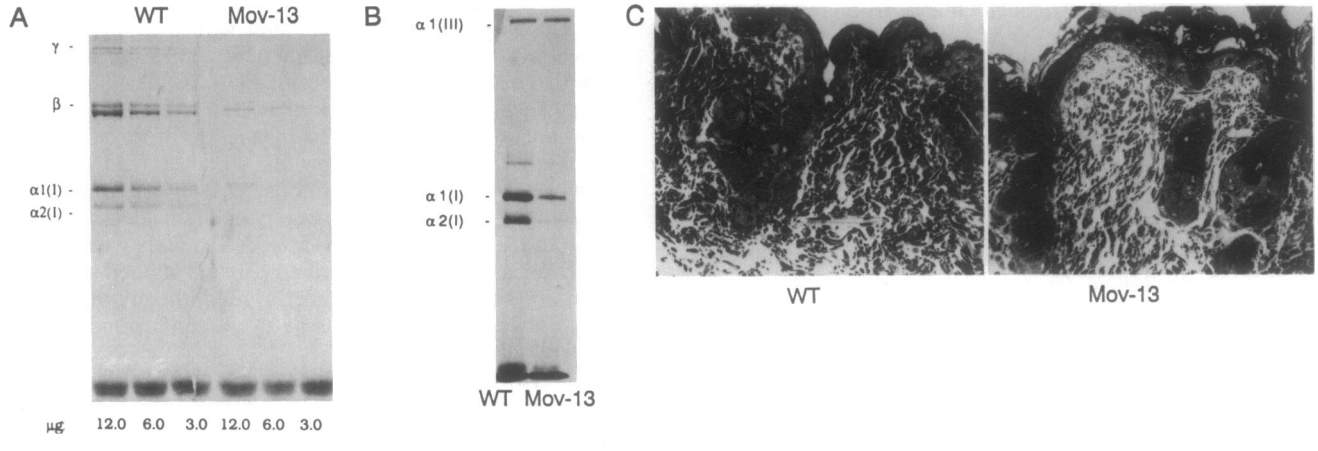

FIG. 1. Collagen content of wild-type (WT) and *Mov-13* nonmineralized connective tissue (skin). (*A*) Total protein extracts from the skin of 15-week-old wild-type and *Mov-13* female littermates were prepared, and protein quantitation was performed as described. Equal protein aliquots were treated with pepsin (100 μg/ml) and then lyophilized prior to electrophoretic separation. Serial 1:1 dilutions (12.0–3.0 μg) of aliquots of wild-type and *Mov-13* samples were separated on a SDS/5% polyacrylamide gel and stained with silver. Type I collagen migrated as α, β, and λ forms because of the presence of nonreducible crosslinks (in β and λ forms) in skin tissue (24). It is likely that a portion of the noncollagenous skin protein degraded by pepsin treatment migrated near the bottom of the gel as silver-stained bands of varying intensity. (*B*) Collagen production by primary skin fibroblast cultures established from 15-week-old wild-type and *Mov-13* female mice is shown. The experiment was standardized according to cell number and normalized based on the established relationship between production of *Mov-13* types I and III by mouse cells (25). The result shown is representative of three independent labeling experiments: in two experiments, radiolabeled samples were treated with pepsin prior to electrophoresis, and in the third experiment, samples were analyzed without prior pepsin digestion. The figure shows the results of one experiment with pepsin-treated samples. To quantitate, three exposures (2, 8, and 48 hr at −86°C) of a single experiment were made, the collagen signal from all films was determined by scanning gel densitometry, and the results were averaged [α1(I)/α2(I): wild-type, 2.6:1.0 ± 0.44; *Mov-13*, 2.47:1.0 ± 0.638; the total collagen signal was 30.25 ± 14.28 for wild-type and 15.14 ± 8.63 for *Mov-13*]. (*C*) Representative sections of dermis from 8-week-old wild-type and *Mov-13* male mice are shown. Collagen fibers, oriented both parallel and perpendicular to the plane of section, are more widely separated than normal in the dermis of *Mov-13* mice.

hydroxyproline) was reduced by ≈50% when compared with age- and sex-matched wild-type mice (Table 1). Gender-matched controls were necessary here because of established differences in the collagen content of skin from male and female C57BL mice (28). Type I collagen produced by *Mov-13* cells appeared normal in that migration of α1(I) and α2(I) chains was indistinguishable from wild-type (Fig. 1*B*), and the chains were produced in a 2:1 ratio by scanning gel densitometry. Therefore, the results from four independent experiments indicate that *Mov-13* mice have a nonmineralized connective tissue defect related primarily to reduced amounts of type I collagen.

Whole-bone specimens and microspecimens of cortical bone were used to estimate the structural integrity of mineralized connective tissue (22). Intact long bones (humerus and femur) were tested in a four-point bending apparatus by stressing the specimens to failure and then assessing the ultimate failure load, energy to failure, and stiffness (Fig. 2 *A–D*) (30). *Mov-13* humeri were more fragile than wild type by both failure-load and energy-to-failure criteria (Fig. 2 *A* and *B*). *Mov-13* femurs showed a similar degree of fragility in terms of the energy to failure. Fig. 2*D* depicts the behavior of wild-type and *Mov-13* humeri during four-point bending. At maximum load, the wild-type humerus typically fractured only one cortical surface (in tension), and the fracture then was propagated along the medullary canal. In contrast, the *Mov-13* humerus shattered at maximum load—i.e., immediately broke both cortices. Similar results were obtained with wild-type and *Mov-13* femurs (not shown). The results in Fig. 2*D* provide evidence of the abnormally brittle nature of *Mov-13* bones.

When taken together, the whole-bone data indicate a significant difference in the load deformation response of *Mov-13* bones at failure. In contrast, a significant difference in the stiffness of these samples was not seen (Fig. 2*C*). Stiffness is a measure of preyield behavior. The data suggest, therefore, that the load deformation response of wild-type and *Mov-13* bone was similar prior to failure.

This initial demonstration of bone fragility could have resulted from a change in the cross-sectional geometry of bone or from a change in cortical bone matrix composition. To begin to discriminate between these possibilities, the modulus of elasticity (22) of cortical bone microspecimens was determined (Fig. 2*E*). *Mov-13* microspecimens (milled from the diaphysis of the humerus and femur) consistently displayed a lower modulus, indicating that the composition of *Mov-13* cortical bone likely contributes to bone fragility.

Table 1. Collagen content of wild-type and *Mov-13* skin

Mouse dermal samples	Collagen, μg/mm²
Female	
Mov-13	25.5, 27.3
Wild-type	49.4 ± 3.3 (n = 6)
Male	
Mov-13	50.6, 46.8
Wild-type	110.2 ± 26.2 (n = 6)

The collagen content of dermal samples taken from 8-week wild-type and *Mov-13* mice was calculated based on an assay of total hydroxyproline as described. Collagen content of wild-type samples is given as a mean value (μg of collagen per mm² of the original biopsy) ± SD, and the number of replicate analyses is shown in parentheses. The results shown are representative of three similar experiments. Note: the observed difference in the collagen content of skin samples from male and female wild-type mice is consistent with previous observations in C57BL mice (28) and humans (29). Despite these differences in overall collagen content, a 50% reduction was observed in both male and female *Mov-13* skin samples relative to age- and gender-matched wild-type samples.

Histological analysis supported the observation that *Mov-13* cortical bone is disorganized (Fig. 2*F*). Within the diaphysis of humerus and femur, well-demarcated normal and abnormal regions of cortical bone were identified. The abnormal cortex stained less intensely than normal, and bone cells within this region were not organized in a normal osteonal pattern. Polarized light microscopy demonstrated the regional disorganization of collagen within the cortex. When taken together, the structural and functional data presented in Fig. 2 provide evidence of the decreased mechanical and material properties of *Mov-13* long bones.

Evoked auditory brainstem responses were used to measure hearing sensitivity. A total of four wild-type and six *Mov-13* animals were evaluated. *Mov-13* mice demonstrated a progressive deficit with age (Fig. 3). At 8 and 11 weeks, mutant mice were 10-35 decibels (dB) less sensitive. At 15 weeks, further decreases in sensitivity of ≈20–30 dB were observed. Significantly, in 15-week *Mov-13* animals, no response could be elicited within the frequency range tested (2.0–20.0 kHz) at the limits of the acoustic delivery system [≈110–120 dB SPL (sound pressure level)].

Finally, the external character of *Mov-13* mice, including tooth morphology and mineralization, was analyzed. No evidence of dentinogenesis imperfecta or short stature was seen in the mutants examined (T.L.S. and J.B., unpublished observations). A lack of tooth pathology is consistent with recent evidence demonstrating that, in contrast to other cell types studied, developing odontoblasts efficiently transcribe and translate the *Mov-13* allele into functional pro-α1(I) chains (31).

DISCUSSION

This study shows that a heterozygous null mutation at the α1(I) collagen locus is associated with (*i*) a reduced amount of collagen in nonmineralized connective tissue, (*ii*) profound and progressive hearing loss, and (*iii*) long bones that have significantly reduced mechanical and material properties. As such, the results support our hypothesis that *Mov-13* mice represent a model of human OI-I. The results also provide strong support for the original hypothesis (32) that a heterozygous null α1(I) collagen allele could produce the OI-I phenotype. A previous study suggested that the principal effect of a heterozygous null α1(I) allele would be to decrease collagen production by 50% but that all of the collagen molecules would have α1(I) and α2(I) chains in a normal stoichiometry (32). In fact, this finding has been observed consistently (ref. 2 and references therein), and it represents the most characteristic biochemical correlate of disease. This correlate was observed with primary skin fibroblast cultures derived from *Mov-13* mice (Fig. 1*B*).

The results reported here indicate that a reduced amount of type I collagen has adverse consequences for fiber structure and the organization and structural integrity of connective tissue. Multiprotein structures such as muscle or the mitotic apparatus are sensitive to mutations that result in the incorporation of an inactive (i.e., structurally altered) protein constituent (33). In contrast, the *Mov-13* mutation may represent an example of a null allele that reduces the amount of one component of a multiprotein structure, in this case extracellular matrix, thereby disrupting its integrity and function because of the imbalance. It is somewhat unusual for a heterozygous null allele to be associated with a dominant phenotype. The heteropolymeric nature of collagen, its ordered assembly with other molecules into fibrils, and the abundance and ordered assembly of fibrils within a connective tissue matrix are relevant considerations in this regard. Perhaps the *Mov-13* mutation is dominant because the imbalance can disrupt more than one step in the biosynthetic pathway as collagen is assembled into connective tissue.

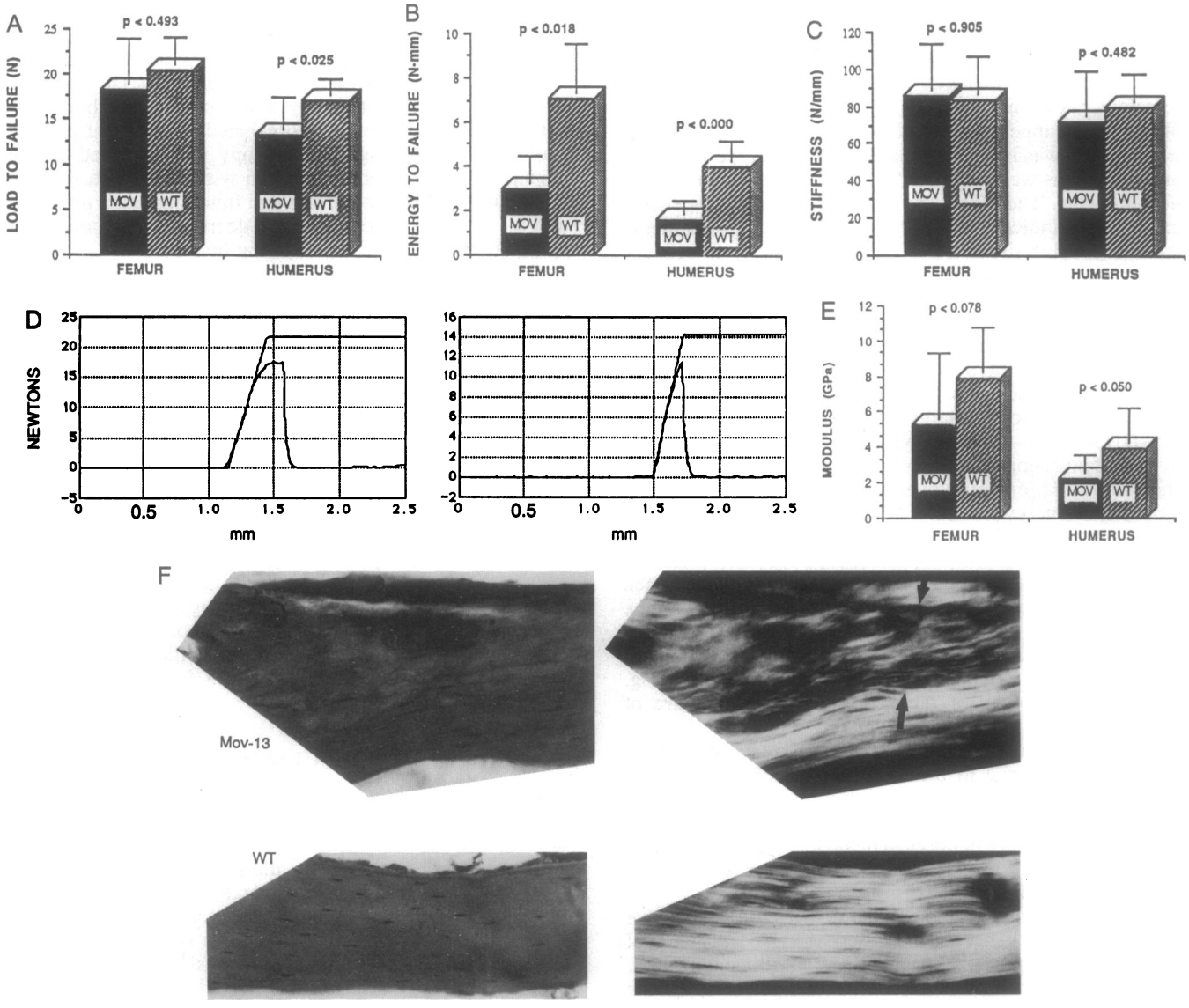

FIG. 2. Assessment of the biomechanical properties and morphology of wild-type and *Mov-13* (MOV) mineralized connective tissue. Long bones were stressed to failure in four-point bending tests. Right humeri and femurs were obtained from seven wild-type (WT) and five *Mov-13* females as described. The mice ranged in age from 6 to 16 weeks, and all comparisons were age-matched. Biomechanical properties (expressed as the mean ± SD) were determined from tests that measured load to failure (*A*), energy to failure (*B*), and stiffness (*C*). Note that within both groups, humeri demonstrated significantly reduced properties when compared with femurs: wild-type, $P = 0.013$ and *Mov-13*, $P = 0.018$. A significant difference in the properties of *Mov-13* femurs was observed despite the generally stronger nature of femoral bones. (*D*) Graphic representation of the behavior of wild-type (*Left*) vs. *Mov-13* (*Right*) humeri during four-point bending. A significant difference in behavior at the maximum load is shown. The graphs are representative of the behavior of all wild-type and *Mov-13* humeri and femurs tested. (*E*) Microspecimen tests. Cortical beam specimens were prepared from left humeri and femurs obtained from wild-type and *Mov-13* mice as described above. Typically, three microspecimens were prepared and tested from each bone. The average of the values obtained from these specimens was then used to calculate modulus (22). (*F*) Microscopy. Bright-field and polarized light images from the diaphyseal cortex of femurs obtained from 8-week wild-type and *Mov-13* femur are shown. *Mov-13* cortical bone was characterized by well demarcated disorganized regions (arrows).

Recently, Kratochwil *et al.* (31) reported that tooth rudiments from embryos of homozygous *Mov-13* mice produce a dentin layer containing normal amounts of type I collagen when grown as transplants either in the anterior chamber of the eye or under the kidney capsule of syngeneic hosts. To account for this unexpected finding, evidence was presented that odontoblasts were able to efficiently produce α1(I) mRNA despite stable integration of the retrovirus within the first intron of the α1(I) collagen gene. In addition, the authors stated that perhaps as many as 5% of osteoblasts from long bone were able to produce normal amounts of type I collagen, thus implying that a small subset of osteoblasts also did not express the mutant phenotype. If this observation can be confirmed, it would suggest that bone tissue mosaicism for expression of the mutant allele may explain why *Mov-13* heterozygotes do not display an obvious mutant phenotype with regard to bone fragility (R.J., unpublished observations). In other words, the effect of the heterozygous null collagen allele on mineralized connective tissues actually may be more severe in the absence of the balancing effect than what was observed in this study.

Type I collagen is thought to make an important contribution to the structure and function of long bone (34). Both the amount and the organization of collagen within the extracellular matrix contribute to the mechanical properties of bone. We reasoned that in addition to modeling a human inherited connective tissue disease, the null collagen mutation harbored by *Mov-13* mice would serve as a useful experimental

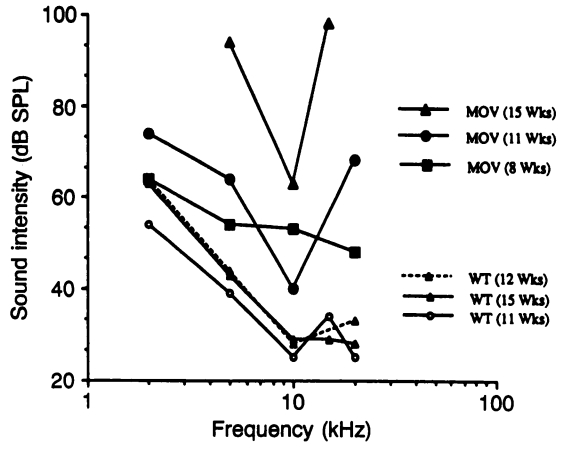

FIG. 3. Auditory brainstem response thresholds to tone bursts of wild-type (WT) and *Mov-13* (MOV) mice as a function of age. Evoked auditory brainstem responses were measured as described. As shown at the bottom of the figure, three wild-type control mice measured at 11, 12, and 15 weeks show no evidence of hearing loss. In contrast, *Mov-13* mice demonstrate profound hearing loss that progressively worsens with time. The figure presents the pattern of hearing loss in one *Mov-13* mouse measured at 8, 11, and 15 weeks. This pattern of hearing loss is representative of similar results obtained with other male (3) and female (1) *Mov-13* mice. SPL, sound pressure level.

probe of collagen's contribution to matrix integrity. The biomechanical tests used in this study allowed us to measure the effect of the mutation at the tissue level.

From the view of biomechanics, bone is considered to be a nonhomogenous composite structure consisting, at the very least, of mineral and organic phases (34). In tests of whole-bone properties, e.g., four-point bending, the sum of the various phases of a composite structure usually contribute to the mechanical properties measured. In other mechanical tests, however, one phase may predominate over another. For example, Burstein *et al.* (35) have shown recently that the mineral phase of bone predominates in the evaluation of pre-yield properties (stiffness). Although more work must be done, the fact that the stiffness of wild-type and *Mov-13* long bone did not differ significantly suggests that the reduced properties of *Mov-13* long bone are based either within the extracellular matrix or in the abdominal interaction between matrix and mineral. Preliminary transmission electron microscopic studies of *Mov-13* long bone support this hypothesis, showing a reduced quantity of collagen fibrils within the cortical bone (femur) of 15-week *Mov-13* mice (M. Lundy and J.B., unpublished observations).

A mouse model corresponding to perinatal lethal OI was created by introducing α1(I) genes carrying point mutations into normal mice (19). This model and the *Mov-13* strain are attractive because they permit the study of connective tissue defects as they evolve under precisely defined conditions. *Mov-13* mice provide an opportunity to investigate the pathology that results from putative null α1(I) mutations in human patients. The strain also represents an experimental system to test therapies designed to strengthen both mineralized and nonmineralized connective tissues. Since *Mov-13* mice share many features of OI-I, the successful strategy may be applicable to this patient population. Given the effect of the *Mov-13* mutation on bone mechanical properties and hearing, such a strategy also may be applicable to other human manifestations of bone disease such as osteoporosis and otosclerosis.

We are grateful to J. Kuhn for thoughtful discussion of this work as it progressed, to L. Smith for help with the skin reference, to J. Lowe for review of the manuscript, and to R. Stone for careful preparation of the manuscript. This work was supported in part by grants from the National Institutes of Health, the Arthritis Foundation, the American Otological Society, and the National Health and Medical Research Council of Australia.

1. Sillence, D. O. (1981) *Clin. Ortho. Relat. Res.* **159**, 11–25.
2. Byers, P. H. (1989) in *The Metabolic Basis of Inherited Diseases*, eds. Scriver, C. R., Beaudet, A. L., Sly, W. S. & Valle, D. (McGraw-Hill, New York), pp. 2805–2842.
3. Paterson, C. R., McAllion, S. & Stellman, J. L. (1984) *N. Engl. J. Med.* **310**, 1694–1696.
4. Shapiro, J. R., Pinkus, A., Weiss, G. & Rowe, D. W. (1982) *J. Am. Med. Assoc.* **247**, 2120–2126.
5. Levin, L. S., Salinas, C. F. & Jorgensen, R. J. (1978) *Lancet* **i**, 332–333.
6. Byers, P. H. & Bonadio, J. F. (1989) in *Collagen: Molecular Biology*, eds. Olsen, B. R. & Nimmi, M. (CRC, Boca Raton, FL), Vol. 4, pp. 125–140.
7. deVries, W. N. & deWet, W. J. (1986) *J. Biol. Chem.* **261**, 9056–9064.
8. Starman, B. J., Eyre, D., Charbonneau, H., Harrylock, M., Weiss, M. A., Weiss, L., Graham, J. M. & Byers, P. H. (1989) *J. Clin. Invest.* **84**, 1206–1214.
9. Nicholls, A. C. & Pope, F. M. (1984) *Br. Med. J.* **288**, 112–113.
10. Steinmann, B. A., Nicholls, A. C. & Pope, F. M. (1986) *J. Biol. Chem.* **261**, 8958–8964.
11. Cohn, D. H., Apone, S., Eyer, D., Starman, B. J., Andreassen, P., Charbonneau, H., Nicholls, A. C., Pope, F. M. & Byers, P. H. (1988) *J. Biol. Chem.* **263**, 14605–14607.
12. Willing, M. C., Cohn, D. H. & Byers, P. H. (1990) *J. Clin. Invest.* **85**, 282–290.
13. Schnieke, A., Harbers, K. & Jaenisch, R. (1983) *Nature (London)* **304**, 315–320.
14. Harbers, K., Kuehn, M., Delius, H. & Jaenisch, R. (1984) *Proc. Natl. Acad. Sci. USA* **81**, 1504–1508.
15. Hartung, S., Jaenisch, R. & Breindl, M. (1986) *Nature (London)* **320**, 365–367.
16. Jahner, D. & Jaenisch, R. (1985) *Nature (London)* **314**, 594–597.
17. Breindl, M., Harbers, K. & Jaenisch, R. (1984) *Cell* **38**, 9–16.
18. Lohler, J., Timpl, R. & Jaenisch, R. (1984) *Cell* **38**, 597–607.
19. Stacey, A., Bateman, J., Choi, T., Mascara, T., Cole, W. G. & Jaenisch, R. (1988) *Nature (London)* **322**, 131–136.
20. Bonadio, J. F., Holbrook, K. A., Gelinas, R. E., Jacob, J. & Byers, P. H. (1985) *J. Biol. Chem.* **260**, 1734–1742.
21. Bateman, J. F., Chan, D., Mascara, T., Rogers, J. G. & Cole, W. G. (1986) *Biochem. J.* **240**, 699–708.
22. Kuhn, J. L., Goldstein, S. A., Choi, K., London, M., Feldkamp, L. A. & Matthews, L. S. (1989) *J. Orthop. Res.* **7**, 876–884.
23. Jewett, D. L. (1970) *Electroencephalogr. Clin. Neurophysiol.* **28**, 609–618.
24. Miller, E. J. (1984) in *Extracellular Matrix Biochemistry*, eds. Piez, K. H. & Reddi, A. H. (Elsevier, New York), pp. 41–81.
25. Liau, G., Yamada, Y., and de Crombrugghe, B. (1985) *J. Biol. Chem.* **260**, 531–535.
26. Dziadek, M., Timpl, R. & Jaenisch, R. (1987) *Biochem. J.* **244**, 375–379.
27. Kratochwil, K., Dziadek, M., Lohler, J. & Jaenisch, R. (1986) *Dev. Biol.* **117**, 596–606.
28. Dickerson, J. W. T. & John, P. M. V. (1964) *Biochem. J.* **92**, 364–368.
29. Shuster, S., Black, M. M. & McVitie, E. (1975) *Br. J. Derm.* **93**, 639–643.
30. Martens, M., Van Audekercke, R., Delport, P., DeMeester, P. & Muelier, J. C. (1983) *J. Biomechanics* **16**, 971–983.
31. Kratochwil, K., von der Mark, K., Kollar, E., Jaenisch, R., Mooslehner, M., Schwarz, M., Haase, K., Gmachl, I. & Harbers, K. (1989) *Cell* **57**, 807–816.
32. Barsh, G. A., David, K. E. & Byers, P. H. (1982) *Proc. Natl. Acad. Sci. USA* **79**, 3838–3842.
33. Herskowitz, I. (1987) *Nature (London)* **329**, 219–222.
34. Martin, R. B. & Burr, D. B. (1989) *Structure, Function, and Adaptation of Compact Bone* (Raven, New York), pp. 57–84.
35. Burstein, A. H., Zika, J. M., Heiple, K. G. & Klein, L. (1975) *J. Bone Jt. Surg. Am. Vol.* **57**, 956–961.